A Consensus Model of Human Apolipoprotein A-I in its Monomeric and Lipid-free State

John T. Melchior[1], Ryan G. Walker[2], Allison L. Cooke[1], Jamie Morris[1], Mark Castleberry[1], Thomas B. Thompson[2], Martin K. Jones[3], Hyun D. Song[3], Kerry-Anne Rye[4], Mike N. Oda[5], Mary G. Sorci-Thomas[6], Michael J. Thomas[7], Jay W. Heinecke[8], Xiaohu Mei[9], David Atkinson[9], Jere P. Segrest[3], Sissel Lund-Katz[10], Michael C. Phillips[10], and W. Sean Davidson[1]

Online Supplement

Supplementary Table 1

Identified INTRA-peptide BS^3 and CBDPS cross-links in isolated lipid-free, monomeric apoA-I samples derived from mixed ^{14}N and ^{15}N labeled proteins

Cross-link	Peptides involved[a]	Mod.[b]	X-Linker	Peptide mass[c]		Span
				^{14}N	^{15}N	
				Da		
S87-K88	84-QEM**SK**DLEEVK-94	XL	BS^3	1472.72	1486.68	Intra
		--[d]	--[d]			Intra
K12-K23	11-V**K**DLATVYVDVL**K**DSGR-27	XL	BS^3	2015.14	2037.08	Intra
		XL	CBDPS	2386.15	2408.09	Intra
S55-K59	46-LLDNWDSVT**S**TFS**K**LR-61	XL	BS^3	2019.05	2040.98	Intra
		XL	CBDPS	2390.09	2412.04	Intra
K94-K96	89-DLEEV**K**A**K**VQPYLDDFQK-106	XL	BS^3	2302.20	2325.13	Intra
		XL	CBDPS	2673.24	2696.18	Intra
K133-K140	132-Q**K**LHELQE**K**LSPLGEEMR-149	XL	BS^3	2302.22	2329.14	Intra
		XL	CBDPS	2673.26	2700.18	Intra
K206-K208	196-ATEHLSTLSE**K**A**K**PALEDLR-215	XL	BS^3	2346.26	2373.18	Intra
		XL	CBDPS	2717.30	2744.22	Intra
K140-S142	132-QKLHELQE**K**L**S**PLGEEMR-149	XL,H	BS^3	2458.30	2485.23	Intra
		--[d]	--[d]			--[d]
S36-K40	28-DYVSQFEG**S**ALG**K**QLNLK-45	--[d]	--[d]			--[d]
		XL	CBDPS	2505.15	2528.11	Intra
K106-K107	97-VQPYLDDFQ**KK**WQEEMELYR-116	XL	BS^3	2782.36	2811.28	Intra
		--[d]	--[d]			--[d]
K52-K59		--[d]	--[d]			--[d]
	46-LLDNWD**S**VTSTFS**K**LR-61	XL	CBDPS	2390.09	2412.04	Intra

[a] Lysines or serines involved in cross-links are in bold.

[b] Chemical modifications: XL = 1 complete cross-link (BS^3 +138.06808 Da, CBDPS +509.09682 Da), H = 1 hydrolyzed cross-linker (BS^3: +156.07864 Da, CBDPS: +527.10738 Da).

[c] Experimentally derived monoisotopic mass for each peptide with each isotope and the combinations.

[d] Not detected. These ions were detectable in one sample set; for example CBDPS but not BS^3.

Supplementary Table 2

Identified INTER-peptide BS³ and CBDPS cross-links in isolated lipid-free, monomeric apoA-I samples derived from mixed ^{14}N and ^{15}N labeled proteins

Cross-link	Peptides involved[a]	Mod.[b]	X-Linker	Peptide mass[c]		Span
				^{14}N	^{15}N	
				Da		
K118-K239	117-Q**K**VEPLR-123	XL	BS³	1608.93	1628.87	Intra
	239-**K**LNTQ-243	XL	CBDPS	1319.98	1999.93	Intra
K94-K239	89-DLEEV**K**AK-96	XL	BS³	1670.93	1688.88	Intra
	239-**K**LNTQ-243	XL	CBDPS	2041.96	2059.91	Intra
K133-K239	132-Q**K**LHELQEK-140	XL	BS³	1892.06	1914.99	Intra
	239-**K**LNTQ-243	XL	CBDPS	2263.09	2286.03	Intra
K182-K239	178-LEAL**K**ENGGAR-188	XL	BS³	1897.04	1920.97	Intra
	239-**K**LNTQ-243	XL	CBDPS	2268.08	2292.01	Intra
NT-239	-1-**G**DEPPQSPWDR-10	XL	BS³	2022.98	2046.92	Intra
	239-**K**LNTQ-243	XL	CBDPS	2394.02	2417.96	Intra
K118-S142	117-Q**K**VEPLR-123	XL	BS³	2037.11	2061.04	Intra
	141-L**S**PLGEEMR-149	XL	CBDPS	2408.15	2432.08	Intra
S167-K239	161-THLAPY**S**DELR-171	XL	BS³	2041.07	2065.00	Intra
	239-**K**LNTQ-243	XL	CBDPS	2412.13	2432.09	Intra
S87-K239	84-QEM**S**KDLEEVK-94	XL	BS³	2075.06	2097.00	Intra
	239-**K**LNTQ-243	XL	CBDPS	2446.10	2468.04	Intra
K107-K239	107-**K**WQEEMELYR-116	XL	BS³	2151.09	2175.02	Intra
	239-**K**LNTQ-243	XL	CBDPS	2522.13	2546.06	Intra
K118-K133	117-Q**K**VEPLR-123	XL	BS³	2158.23	2185.15	Intra
	132-Q**K**LHELQEK-140	XL	CBDPS	2529.28	2556.20	Intra
K118-K182	117-Q**K**VEPLR-123	XL	BS³	2163.23	2191.15	Intra
	178-LEAL**K**ENGGAR-188	XL	CBDPS	2534.26	2562.18	Intra
K96-K239	95-A**K**VQPYLDDFQK-106	XL	BS³	2191.17	2215.10	Intra
	239-**K**LNTQ-243	XL	CBDPS	2562.21	2586.14	Intra
K12-K239	11-V**K**DLATVYVDVLK-23	XL	BS³	2202.27	2225.21	Intra
	239-**K**LNTQ-243	--[d]	CBDPS	--[d]	--[d]	--[d]
NT-K118	-1-**G**DEPPQSPWDR-10	XL	BS³	2289.16	2317.08	Intra
	117-Q**K**VEPLR-123	XL	CBDPS	2660.20	2688.12	Intra
K182-K208	178-LEAL**K**ENGGAR-188	XL	BS³	2306.28	2335.20	Intra
	207-A**K**PALEDLR-215	XL	CBDPS	2677.28	2706.20	Intra
NT-K94	-1-**G**DEPPQSPWDR-10	XL	BS³	2351.15	2377.07	Intra
	89-DLEEV**K**AK-96	XL	CBDPS	2722.19	2748.13	Intra
S201-K208	196-ATEHL**S**TLSEK-206	XL	BS³	2364.25	2391.17	Intra
	207-A**K**PALEDLR-215	XL	CBDPS	2735.28	2762.21	Intra
K107-K118	107-**K**WQEEMELYR-116	XL	BS³	2417.26	2445.18	Intra
	117-Q**K**VEPLR-123	XL	CBDPS	2788.30	2816.22	Intra
NT-K208	-1-**G**DEPPQSPWDR-10	XL	BS³	2432.22	2461.13	Intra
	207-A**K**PALEDLR-215	XL	CBDPS	2803.25	2832.17	Intra
K107-K208	107-**K**WQEEMELYR-116	XL	BS³	2560.31	2589.23	Intra
	207-A**K**PALEDLR-215	XL	CBDPS	2931.36	2960.27	Intra
NT-K133	-1-**G**DEPPQSPWDR-10	XL	BS³	2572.27	2603.19	Intra
	132-Q**K**LHELQEK-140	XL	CBDPS	2943.32	2974.23	Intra
NT-K182	-1-**G**DEPPQSPWDR-10	XL	BS³	2577.26	2609.17	Intra
	178-LEAL**K**ENGGAR-188	XL	CBDPS	2948.31	2980.21	Intra
K96-K208	95-A**K**VQPYLDDFQK-106	XL	BS³	2600.40	2629.32	Intra
	207-A**K**PALEDLR-215	XL	CBDPS	2971.45	3000.37	Intra
S58-K239	46-LLDNWDSVTSTF**S**KLR-61	XL	BS³	2621.39	2651.30	Intra
	239-**K**LNTQ-243	XL	CBDPS	2992.43	3022.35	Intra
S59-K239	46-LLDNWDSVTSTFS**K**LR-61	XL	BS³	2621.39	2651.30	Intra
	239-**K**LNTQ-243	XL	CBDPS	2992.44	3022.35	Intra
K140-K239	134-LHELQE**K**LSPLGEEMR-149	XL	BS³	2648.40	2679.31	Intra
	239-**K**LNTQ-243	XL	CBDPS	3019.45	3050.35	Intra
K133-S142	132-Q**K**LHELQEK-140	--[d]	BS³	--[d]	--[d]	--[d]
	141-L**S**PLGEEMR-149	XL	CBDPS	2691.27	2718.19	Intra
K107-K182	107-**K**WQEEMELYR-116	XL	BS³	2705.36	2737.28	Intra
	178-LEAL**K**ENGGAR-188	XL	CBDPS	3076.39	3108.31	Intra
K40-K239	28-DYVSQFEGSALG**K**QLNLK-45	XL	BS³	2736.45	2767.36	Intra
	239-**K**LNTQ-243	--[d]	CBDPS	--[d]	--[d]	--[d]

K96-K182	95-A**K**VQPYLDDFQK-106 178-LEAL**K**ENGGAR-188	XL --[d]	BS^3 CBDPS	2745.44 --[d]	2777.37 --[d]	Intra --[d]
NT-K88	-1-**G**DEPPQSPWDR-10 84-QEMS**K**DLEEVK-94	XL XL	BS^3 CBDPS	2755.28 3126.32	2785.20 3156.25	Intra Intra
K12-K182	11-V**K**DLATVYVDVLK-23 178-LEAL**K**ENGGAR-188	XL XL	BS^3 CBDPS	2756.55 3127.61	2787.46 3158.53	Intra Intra
K107-S167	107-**K**WQEEMELYR-116 161-THLAPY**S**DELR-171	--[d] XL	BS^3 CBDPS	--[d] 3220.44	--[d] 3252.35	--[d] Intra
NT-K96	-1-**G**DEPPQSPWDR-10 95-A**K**VQPYLDDFQK-106	XL XL	BS^3 CBDPS	2871.39 3242.44	2903.29 3274.30	Intra Intra
NT-K12	-1-**G**DEPPQSPWDR-10 11-V**K**DLATVYVDVLK-23	XL XL	BS^3 CBDPS	2882.49 3253.54	2913.40 3284.45	Intra Intra
K96-S167	95-A**K**VQPYLDDFQK-106 161-THLAPY**S**DELR-171	XL XL	BS^3 CBDPS	2889.47 3260.52	2921.38 3292.43	Intra Intra
K118-K140	117-Q**K**VEPLR-123 134-LHELQE**K**LSPLGEEMR-149	XL XL	BS^3 CBDPS	2914.59 3285.62	2949.48 3320.52	Intra Intra
K88-K96	84-QEMS**K**DLEEVK-94 95-A**K**VQPYLDDFQK-106	XL XL	BS^3 CBDPS	2923.47 3294.51	2953.38 3324.46	Intra Intra
S167-K182	161-THLAPY**S**DELR-171 178-LEAL**K**ENGGAR-188	--[d] XL	BS^3 CBDPS	--[d] 2966.39	--[d] 2998.30	--[d] Intra
K96-K107	95-A**K**VQPYLDDFQK-106 107-**K**WQEEMELYR-116	XL XL	BS^3 CBDPS	2999.50 3370.54	3031.40 3402.45	Intra Intra
K40-K118	28-DYVSQFEGSALG**K**QLNLK-45 117-Q**K**VEPLR-123	XL --[d]	BS^3 CBDPS	3002.64 --[d]	3037.52 --[d]	Intra --[d]
K208-K239	196-ATEHLSTLSEKA**K**PALEDLR-215 239-**K**LNTQ-243	XL,H --[d]	BS^3 CBDPS	3104.66 --[d]	3139.56 --[d]	Intra --[d]
K195-K208	189-LAEYHA**K**ATEHLSTLSEK-206 207-A**K**PALEDLR-215	XL XL	BS^3 CBDPS	3176.69 3547.74	3213.59 3584.64	Intra Intra
K40-K133	28-DYVSQFEGSALG**K**QLNLK-45 132-Q**K**LHELQEK-140	XL --[d]	BS^3 CBDPS	3285.75 --[d]	3323.64 --[d]	Intra --[d]
NT-K59	-1-**G**DEPPQSPWDR-10 46-LLDNWDSVTSTFS**K**LR-61	XL XL	BS^3 CBDPS	3301.62 3672.66	3339.50 3710.55	Intra Intra
NT-K140	-1-**G**DEPPQSPWDR-10 134-LHELQE**K**LSPLGEEMR-149	XL,H --[d]	BS^3 CBDPS	3740.87 --[d]	3783.75 --[d]	Intra --[d]
S204-K208	189-LAEYHAKATEHLSTL**S**EK-206 207-A**K**PALEDLR-215	XL,H --[d]	BS^3 CBDPS	3332.78 --[d]	3369.67 --[d]	Intra Intra
K226-K239	216-QGLLPVLESF**K**VSFLSALEEYTK-238 239-**K**LNTQ-243	XL --[d]	BS^3 CBDPS	3337.83 --[d]	3371.75 --[d]	Intra --[d]
K77-K239	62-EQLGPVTQEFWDNLE**K**ETEGLR-83 239-**K**LNTQ-243	XL XL	BS^3 CBDPS	3357.70 3728.74	3395.59 3766.62	Intra Intra
NT-K23	-1-**G**DEPPQSPWDR-10 11-VKDLATVYVDVL**K**DSGR-27	XL,H --[d]	BS^3 CBDPS	3453.76 --[d]	3491.66 --[d]	Intra --[d]
K118-K226	117-Q**K**VEPLR-123 216-QGLLPVLESF**K**VSFLSALEEYTK-238	XL --[d]	BS^3 CBDPS	3604.01 --[d]	3641.90 --[d]	Intra --[d]
K77-K182	62-EQLGPVTQEFWDNLE**K**ETEGLR-83 178-LEAL**K**ENGGAR-188	XL XL	BS^3 CBDPS	3911.98 4283.03	3957.85 4328.88	Intra Intra
NT-K77	-1-**G**DEPPQSPWDR-10 62-EQLGPVTQEFWDNLE**K**ETEGLR-83	XL XL	BS^3 CBDPS	4037.93 4408.97	4083.79 4454.83	Intra Intra
K77-K88	62-EQLGPVTQEFWDNLE**K**ETEGLR-83 84-QEMS**K**DLEEVK-94	XL XL	BS^3 CBDPS	4090.01 4461.03	4133.88 4504.91	Intra Intra
K40-K140	28-DYVSQFEGSALG**K**QLNLK-45 132-QKLHELQE**K**LSPLGEEMR-149	XL,H --[d]	BS^3 CBDPS	4454.36 --[d]	4504.22 --[d]	Intra --[d]

[a] Lysines involved in cross-links are in bold.

[b] Chemical modifications: XL = 1 complete cross-link (BS^3 +138.06808 Da, CBDPS +509.09682 Da), H = 1 hydrolyzed cross-linker (BS^3: +156.07864 Da, CBDPS: +527.10738 Da).

[c] Experimentally derived monoisotopic mass for each peptide with each isotope and the combinations.

[d] Not detected. These ions were detectable in one sample set; for example CBDPS but not BS^3.

Supplementary Table 3

Experimental parameters from SAXS sampling of monomeric apoA-I cross-linked with CBDPS or BS3

ApoA-I Sample	**I(O)[a] (Guinier)**	**R_g[b] (Guinier)**	**Real Space R_g**	**D_{max}[c]**	**Volume**	**DAMMIF NSD[d]**
	cm^{-1}	**Å**	**Å**	**Å**	**$Å^3$**	**Å**
CBDPS						
4.0 mg/ml	603	26	25.29	85	70165	
2.0 mg/ml	301	25.8	25.24	83	68091	0.579 ± 0.032
1.0 mg/ml	149	25.1	25.53	83	70191	
BS^3						
4.0 mg/ml	569	25.95	25.54	88	77337	
2.0 mg/ml	294	25.58	25.25	81	77334	0.596 ± 0.024
1.0 mg/ml	140	27.67	25.24	81	83946	

Supplementary Table 4

Universal cross-linking list across four studies on lipid-free monomeric apoA-I

Residue		Reported[a]				Cross-Linker[b]			Distance[c]
1	2	Silva et al	Pollard et al	Segrest et al	Melchior	MDA	BS3	CBDPS	(Å)
1	12		X	X	X	X	X	X	23
1	23				X		X		28
1	59		X		X		X	X	28
1	77				X		X	X	28
1	88				X		X	X	28
1	94				X		X	X	28
1	96	X			X		X	X	28
1	118		X		X		X	X	28
1	133				X		X	X	28
1	140				X		X		28
1	182				X		X	X	28
1	195			X		X			23
1	208				X		X	X	28
1	239				X		X	X	28
12	23	X	X	X	X	X	X	X	23
12	182				X		X	X	28
12	195		X						28
12	226			X		X			23
12	239				X		X		28
23	59	X	X	X	X	X			23
23	239			X		X			23
36	40				X		X	X	28
40	45	X	X	X		X			23
40	59		X						28
40	94			X		X			23
40	118		X		X		X		28
40	133		X	X	X	X	X		23
40	140		X		X		X		28
40	182		X						28
40	239		X	X	X	X	X		23
45	59		X						28
52	59				X		X	X	28
55	59				X		X	X	28
58	239				X		X	X	28
59	195			X		X			23
59	239			X	X	X	X	X	23
77	88				X		X	X	28
77	182				X		X	X	28
77	195			X		X			23
77	208			X		X			23
77	239				X		X	X	28
87	88				X		X		28
87	239				X		X	X	28
88	94	X	X						28
88	96				X		X	X	28
88	118		X						28
88	195			X		X			23
94	96	X	X	X	X	X	X	X	23
94	226			X		X			23
94	239		X	X	X	X	X	X	23
96	106	X	X						28
96	107				X		X	X	28
96	167				X		X	X	28
96	182				X		X		28
96	195	X		X		X			23
96	208	X		X	X	X	X	X	23
96	226	X							28

96	239				X	X	X	X	X	23
106	107	X			X	X	X	X	X	23
107	118					X		X	X	28
107	167					X			X	28
107	182					X		X	X	28
107	208					X		X	X	28
107	239				X	X	X	X	X	23
118	133			X	X	X	X	X	X	23
118	140	X		X	X	X	X	X	X	23
118	142					X		X	X	28
118	182					X		X	X	28
118	195				X		X			23
118	208				X		X			23
118	226				X	X	X	X		23
118	239				X	X	X	X	X	23
133	140	X		X	X	X	X	X	X	23
133	142					X		X		28
133	239				X	X	X	X	X	23
140	142					X		X	X	28
140	239				X	X	X	X	X	23
167	182					X			X	28
167	239					X		X	X	28
182	195				X		X			23
182	208					X		X	X	28
182	226				X		X			23
182	239					X		X	X	28
195	206				X		X			23
195	208					X		X	X	28
195	226				X		X			23
195	239				X		X			23
201	208					X		X	X	28
204	208					X		X		28
206	208	X		X	X	X	X	X	X	23
206	226				X		X			23
208	239					X		X		28
226	238	X								28
226	239				X	X	X	X		23
238	239	X		X	X		X			23

[a] Cross-linked residues reported in the current study or Silva et al [1], Pollard et al [2], or Segrest et al [3].
[b] Cross-link found with cross-linking reagent
[c] Upper-limit Cα-Cα distance used as cross-linking constraint for consensus model

Supplementary Table 5

Reported structural features of lipid-free monomeric apoA-I determined by far circular dichroism

Author	Year	A-I Source	[PRO] mg/ml	Temp (°C)	Alpha	Beta-Sheet	Coil/ Turns	Ref
Davidson et al	1996	Plasma	0.05-0.1	25	57.0%		43.0%	4
Bergeron et al	1997	Native His-apoA-I	0.067	24	56.0% 50.0%		44.0% 50.0%	5 **a**
Rogers et al	1998	Plasma	0.01-0.56	25	68.0%		32.0%	6 **b**
Sparks et al	1999	Plasma	0.067	24	49.0%		51.0%	7 **c**
Suurkuusk et al	1999	Plasma	0.1	25	44.0%		56.0%	8 **d**
Davidson et al	1999	Pro-apoA-I	0.05-0.1	25	56.0%		44.0%	9 **d**
Huang et al	2000	Pro-apoA-I	0.1	25	45.0%		55.0%	10
Panzenbock et al	2000	Plasma	0.1	25	52.0%	7.9%	37.3%	11
Weinberg et al	2000	Plasma	0.08	25	54.0%		46.0%	12
Sigalov et al	2001	Plasma	0.1	25	62.0%		38.0%	13
Gorshkova et al	2002	Pro-apoA-I	0.025-0.1	25	58.0%		42.0%	14 **d**
Reschly et al	2002	Plasma	0.1	25	40.0%		60.0%	15
Saito et al	2003	Plasma r-apoA-I	0.025-0.05	25	49.0% 46.0%		51.0% 54.0%	16 **e**
Fang et al	2003	Plasma r-apoA-I	0.06-0.1	25	60.0% 55.0%		40.0% 45.0%	17 **f**
Saito et al	2004	Plasma r-apoA-I	0.025	25	46.0% 44.0%		54.0% 56.0%	18 **e**
Han et al	2005	r-apoA-I	0.07	25	52.0%		48.0%	19 **d**
Silva et al	2005	Plasma	0.03	25	55.0%	8.0%	37%	1
Zhu et al	2005	His-apoA-I	0.06-0.1	25	54.0%		46.0%	20 **a**
Arnulphi et al	2005	Plasma	0.054	15 37	48.0% 50.0%		52.0% 50.0%	21
Gorshkova et al	2006	Pro-apoA-I	0.025-0.08	25	58.0% 59.0%		42.0% 41.0%	22 **g**
Tanaka et al	2008	r-apoA-I	0.05	25	44.0%		56.0%	23 **d**
Fukuda et al	2008	Plasma	0.06	37	44.0%		56.0%	24
Kono et al	2009	r-apoA-I	0.03-0.05		46.0%		54.0%	25 **d**
Chetty et al	2009	Plasma	0.05	25	49.0%		51.0%	26
Jayaraman et al	2012	Plasma	0.02	25	57.0%		43.0%	27
Zehender et al	2012	r-apoA-I	0.1	25	45.0%		55.0%	28 **h**
Della-Riva et al	2013	r-apoA-I	0.1	25	56.0%		44.0%	29 **i**

[a] Studies performed on recombinant human apoA-I which contains Met-Arg-Gly-Ser-$(His)_6$ on the NT

[b] CD was obtained on a range of values that both fall within and exceed concentrations reported for monomeric apoA-I .

[c] The source of apoA-I is unclear. "Lyophilized apoA-I (purity > 96%) were purchased from Biogenesis."

[d] Studies performed on recombinant human proapoA-I which contains a hexapeptide on the NT normally cleaved when secreted into plasma.

[e] Studies performed on recombinant human apoA-I which containing a Gly-Ser, on the NT.

[f] Studies performed on recombinant human apoA-I containing a Gly-Ala-Met-Gly-Ser, on the NT.

[g] Studies performed on recombinant human proapoA-I containing a hexapeptide on the NT normally cleaved when secreted into plasma. Protein was expressed in either a baculovirus (top) or adenovirus (bottom) system.
[h] Studies performed on recombinant human apoA-I containing a Gly-Gly on the NT.
[i] Studies performed on recombinant human apoA-I which contains a point mutation, E2D at the N-terminus.

Supplementary Table 6

Reported cleavage sites on lipid-free monomeric apoA-I determined by limited proteolysis

Author	Year	A-I Source	[PRO] mg/ml	Temp (°C)	Proteolytic Enzyme	Cleavage Sites	Ref
Roberts et al	1997	Plasma	0.1	37	a,b	Y115, E125, E136, E191, Y192, L200, L211, E212, E223, F225, E235	30
Rogers et al	1997	Plasma	0.1	37	a	F57, L122, Y192	31

[a] Chymotrypsin: Cleaves at the carboxy-terminal side of Tyrosine (Tyr, Y), Phenalanine (Phe, F), Tryptophan (Trp,W), and Leucine (Leu, L).
[b] *S. Aureus* V8 protease: Cleaves at the carboxy-terminal side of glutamic acid (Glu, E) residues

Supplementary Table 7

Reported molecular dimensions for lipid-free monomeric apoA-I measured by sedimentation velocity

Author	Year	A-I Source	[PRO] mg/ml	Length (Å)	Width (Å)	Axial Ratio	Ref
Barbeau et al	1979	Plasma	0.05-0.7	151.2	25.2	6.0	[32]
Edelstein et al	1980	Plasma	0.05	164	25	6.6	[33]
Rogers et al	1998	Plasma	0.1-0.2	168	24	7.2	[31]

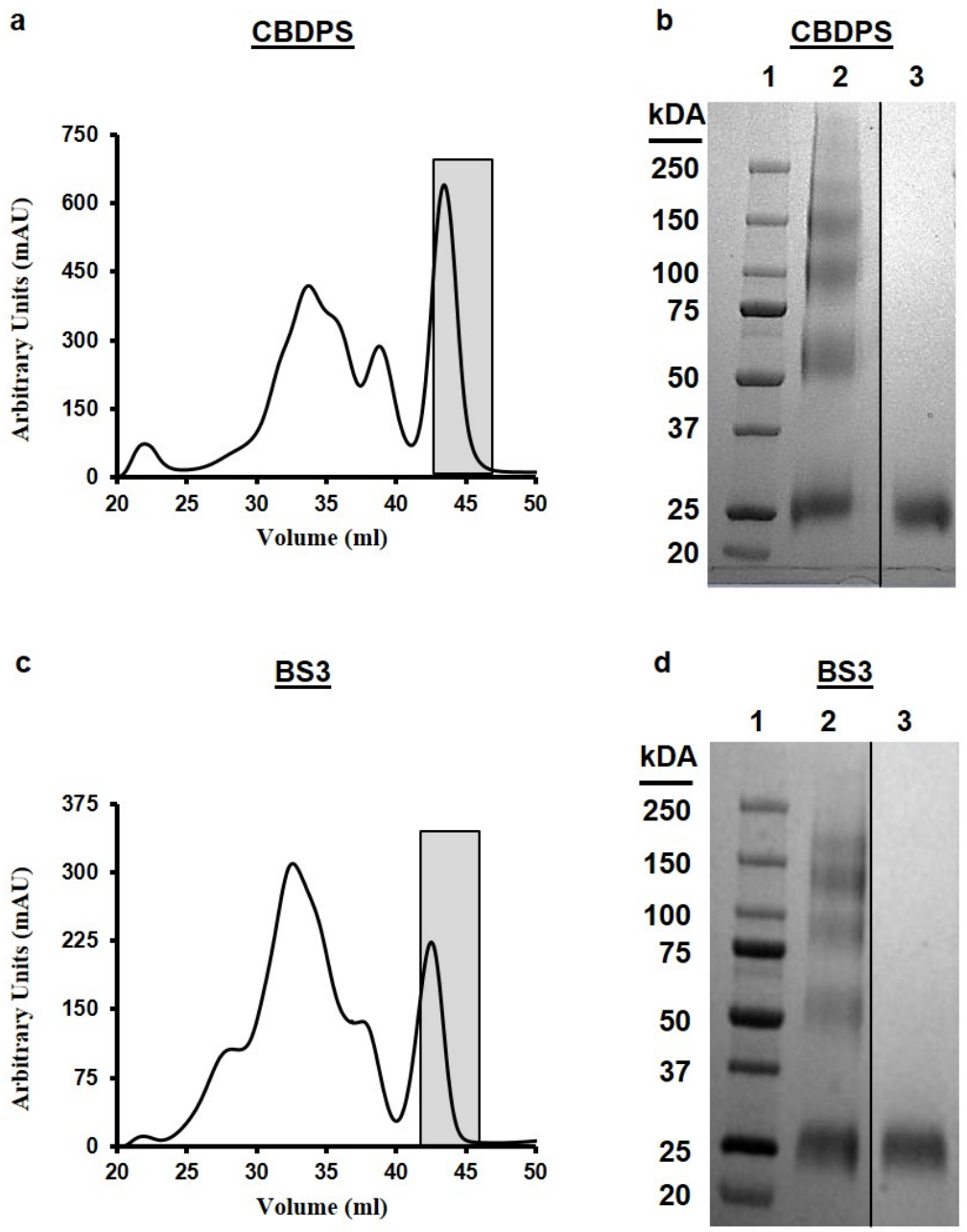

Supplementary Figure 1. Separation and purification of lipid-free apoA-I monomer by gel filtration chromatography. ApoA-I was cross-linked and subjected to gel-filtration chromatography and fractions corresponding to the stable monomeric species were pooled. Chromatograms of apoA-I cross-linked with CBDPS and BS^3 are shown in panels (a) and (c), respectively. The shaded area represents the fractions corresponding to monomeric apoA-I that were pooled for cross-linking and SAXS analysis. Corresponding SDS-PAGE analysis of lipid-free apoA-I cross-linked with CBPDS and BS^3 are shown in panels (b) and (d), respectively. Molecular weight markers are shown in lane 1, cross-linked apoA-I prior to separation is shown in lane 2, and cross-linked monomeric apoA-I after separation is shown in lane 3. Gels were stained with coomassie blue.

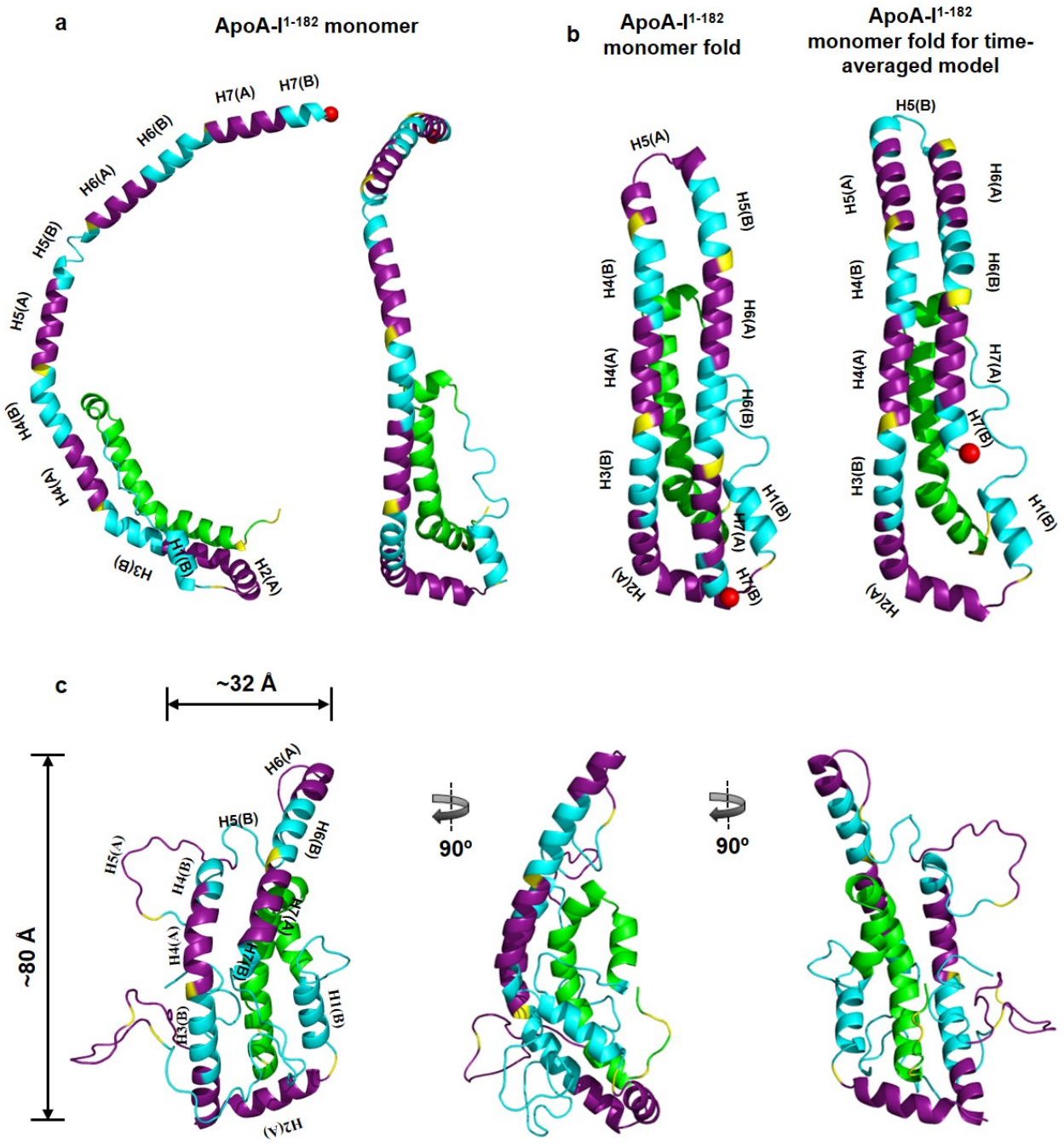

Supplementary Figure 2. Derivation of an all atom model of full-length, lipid-free monomeric apoA-I. Panel (a) shows a single molecule from the reported crystal structure of the apoA-I$^{1-184}$ dimer. Panel (b) shows the folding of helix 6 previously proposed by Mei et. al.[34], and the fold of helix 6 used for the time-averaged structure (right). Panel (c) shows the final time-averaged model. Molecules are colored as previously defined by Mei et. al.[34]. Purple and cyan represent consensus sequence peptide A and B homology sequences, green represents exon-3-encoded region (residues 1-43) and yellow are prolines.

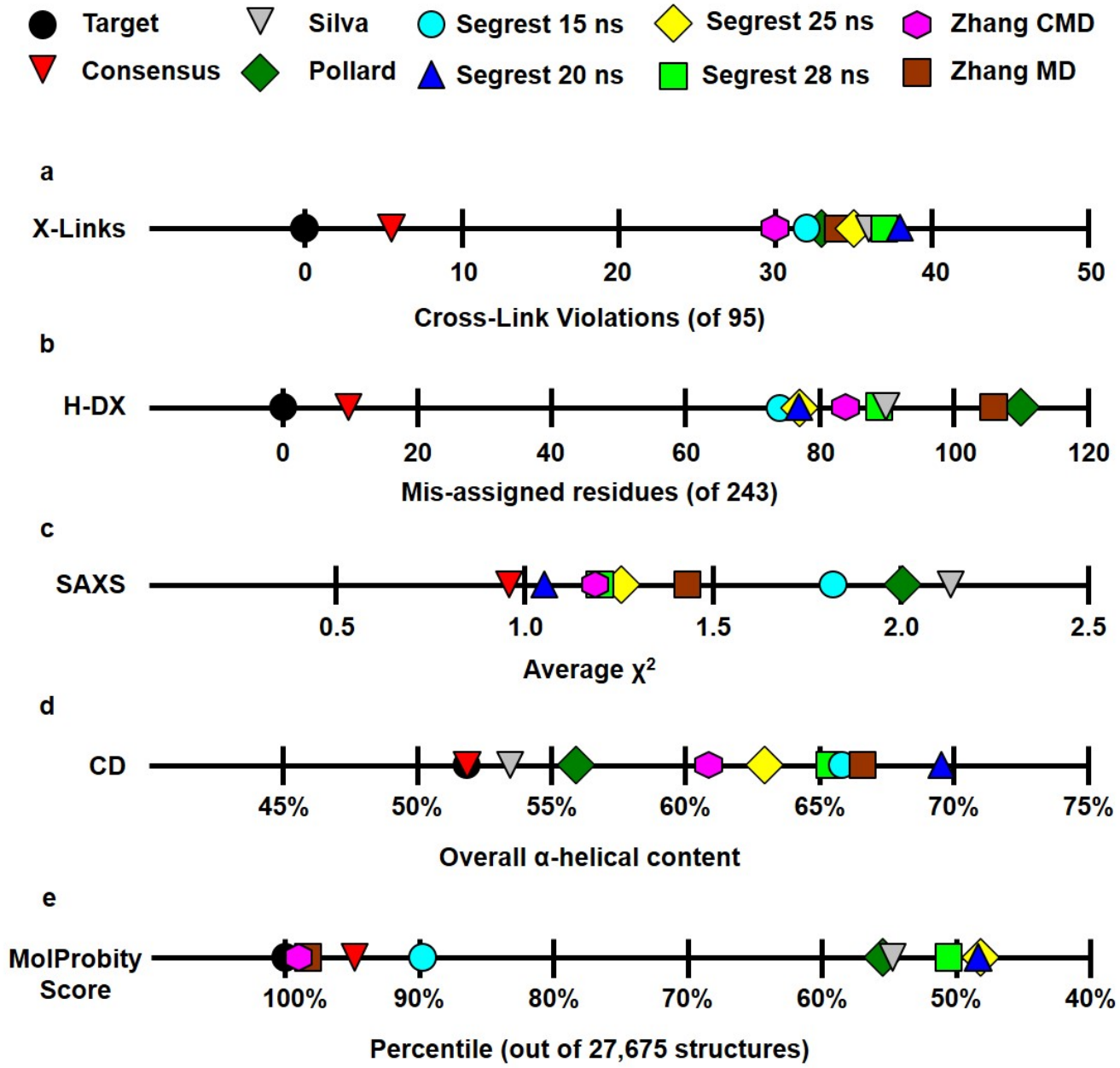

Supplementary Figure 3. Comparison of the newest model to previous models with respect to various pieces of experimental data. The line diagrams show the fit of the models relative to the target value (black circle) derived from current and previous data on lipid-free monomeric apoA-I. Panel (a) shows the model fits to experimental cross-links from the universal cross-linking list (**Supplemental Table 4**) with the target being zero violations. Panel (b) shows the model fits to experimental H-DX data[26] with the target being zero violations. Panel (c) shows the averaged χ^2 values for all models fit to the scattering profiles derived from apoA-I cross-linked with BS^3 and CBDPS. The target for SAXS is the lowest χ^2 value possible with lower values indicating better fits to the experimental scattering curve. Panel (d) shows the fits to overall α-helical data derived values reported across 27 studies as shown in **Supplementary Table 5**. Panel (e) shows the rank of the MolProbity score of all reported models of apoA-I relative to 27,675 crystal structures reported in the protein database.

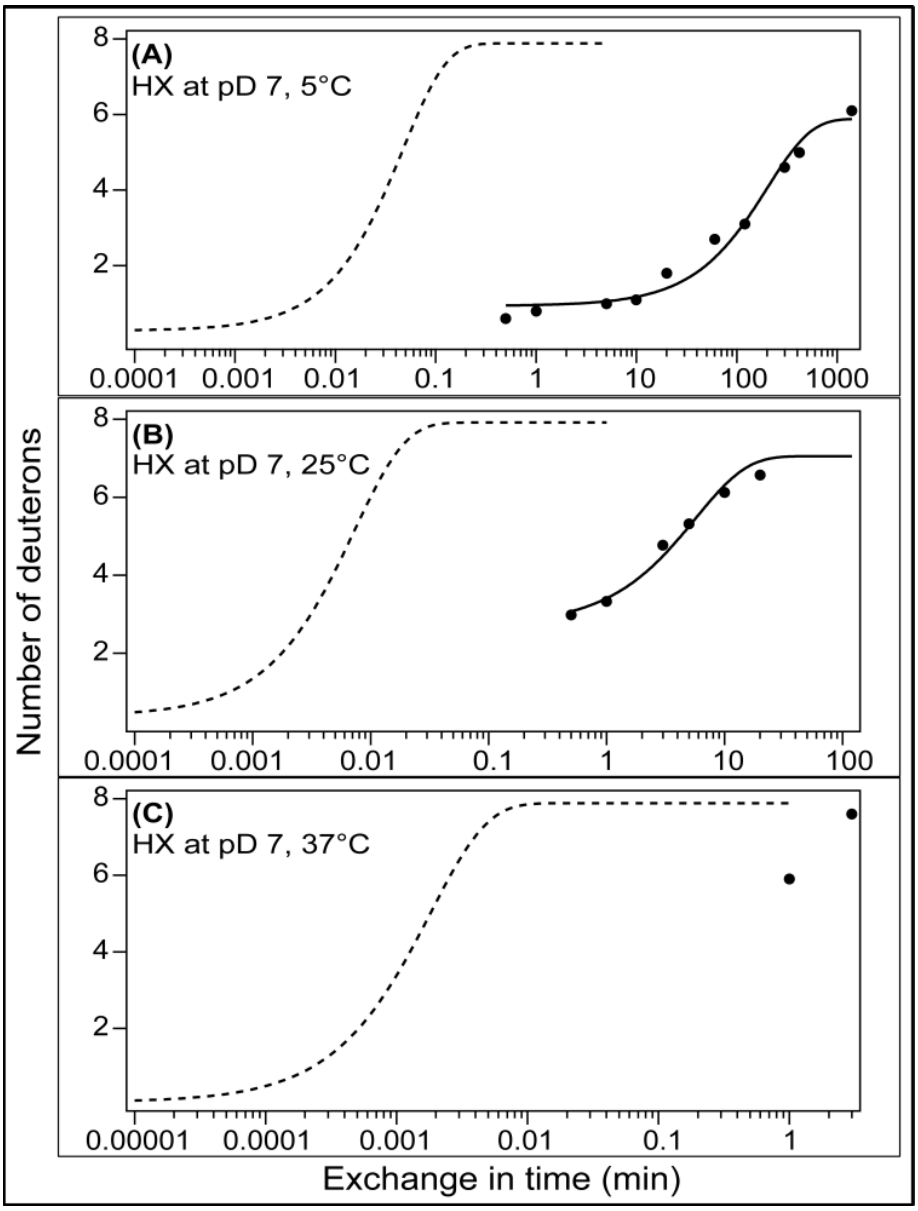

Supplementary Figure 4: Effect of temperature on H-DX in lipid-free apoA-I. The plots compare the measured H-DX kinetics of the apoA-I peptide 159-169 from a helical region at pD 7 and **(A)** 5°C, **(B)** 25°C and **(C)** 37°C to the rate for the peptide in a dynamically disordered state (dashed line). Comparison of the rate constants derived by fitting the dashed and solid time-courses to mono-exponential rate equations yields the protection factor (Pf) and hence the free energy (ΔG) of helix stabilization. After correcting for the effect of temperature on the intrinsic chemical HX rate, the apparent ΔG of helix stability at 5^0C and 25^0C is 5.3 and 3.8 kcal/mol, respectively. The helix stability is less at 37^0C and H-D exchange is complete in ~3 min. [From [26]]

Supplementary Note

Due to space restrictions of the Journal, we were asked to abbreviate our discussion of the model in the main paper. What follows is the original, more complete discussion.

Consistency with previously reported data. Analytical ultracentrifugation (AUC) can provide low-resolution molecular shape information. **Supplementary Table 7** summarizes three analytical ultracentrifugation studies[31-33] on lipid-free apoA-I, which conclude that monomeric apoA-I is asymmetrical in shape with an axial ratio of ~6.5 (161 x 24 Å). This contrasts with our SAXS envelopes which had an axial ratio of 2.1-2.8. The discrepancy between AUC and SAXS measurements may reflect the dynamics of apoA-I in solution vs the 'locked' state after cross-linking. Using Forster resonance energy transfer, Brouillette and colleagues later concluded apoA-I is more compact[35] and that the AUC results[31] were probably reflective of an unfolded protein due to high external centrifugal forces. The molecular length measured by AUC is about double what we measured by SAXS while the width is about half. This is consistent with the notion that monomeric apoA-I, like apoA-IV[36], can open up like a pocket knife to oligomerize or bind lipids. This may be further supported by EPR studies identifying residues 26, 44, 64, 167, 217, and 226 to be in the same plane[37]. In the time-averaged structure all but residues 217 and 226 fall within the same plane. Given that EPR studies were executed on multimeric apoA-I, it's plausible that when H6 opens and apoA-I self-associates, residues 217 and 226 fall in-plane with the remaining residues. Several laboratories[38-40] have suggested that helix 5 may be the center of such a hinge. Additionally, the positioning of H6 on the new model appears poised to unfold for interaction with lipid or another molecule. The exact nature of this unfolding must await further studies focused specifically on apoA-I oligomerization.

Limitations of the model. A limitation of the current model stems from our attempt to represent a highly dynamic protein with a single, time-averaged model. Numerous studies have documented the "molten globule" nature of apoA-I[16,41]. H-DX quantifies the rate of proton transfer to amide groups in the protein and allows one to determine locations and stabilities of elements of secondary structure[26]. Given that the observed rate constant for hydrogen exchange is lower than the rate constant for helical closing and H-bond formation in apoA-I, the observed hydrogen exchange rate is related to the α-helix open-closed equilibrium constant (K_{op}), a measure of the free energy (ΔG) of helix stabilization. This concept is illustrated in **Supplementary Figure 4** which compares hydrogen-exchange rates at three temperatures for a peptide segment in an unprotected random coil state (dashed line) and in a protected helical state (solid line). Given the degree of protection, expressed as the protection factor P_f (=1/K_{op}), one can derive K_{op} and the ΔG of helix stabilization. ApoA-I has ΔG of helix stabilization ranging from ~3-5 kcal/mol[26]. At neutral pH and room temperature, P_f for these helices is ~$10e^4$, which corresponds with complete hydrogen exchange into the α-helical segments occurring in ~10 minutes (**Supplementary Figure 4B**); i.e. all the helical segments of native apoA-I have opened and closed at least once in this timeframe. To put this in context, a more stable globular protein such as cytochrome C has a ΔG of helix stabilization of 10 kcal/mol corresponding to a P_f of ~$10e^8$, indicating that complete hydrogen exchange would require ~10 weeks. Given this degree of secondary structure dynamics, the overall high content of random coil, and the number of solvent exposed hydrophobic residues in apoA-I, it may not be possible to fully capture apoA-I structure in a single model. At physiological temperatures, apoA-I may adopt many of the structures shown in **Fig. 1**. However, our model is a time-averaged structure derived from experimental data obtained on a time scale that is much longer than typical secondary structure oscillations. For this reason, we think of it as a base model upon which hypothesized dynamics and conformational alterations can be further tested or modeled.

Another issue relates to the notion of solvent accessibility of the cross-linking reagents. While most cross-links fit the model in terms of Euclidian distance ('as the crow flies'), nearly half are impeded by some obstruction. For example, the cross-link path may be sterically hindered by a side chain rotamer from a non-participating residue or it may pass through the backbone of an adjacent helical domain. The answer to how this can happen most likely lies in protein dynamics. Cross-linking experiments are

completed on the time scale of minutes to hours, substantially longer than the timescale described above for helix opening and closing. Thus, α-helical domains in apoA-I have unfolded and refolded multiple times allowing cross-linker access to amines that are otherwise inaccessible. Furthermore, it is possible that cross-links may stabilize low probability structures, which would facilitate these observations. However, previous reports have shown excellent consistency between observed cross-links on solution structures with crystal structures of apoA-I$^{1\text{-}184\ (42)}$ and apoA-IV[36] and non-apolipoproteins[43-46] validating the approach. It's important to recognize that *in vitro* studies presented here are performed on an ensemble of structures that vary at any given time point during the experiment. Additionally, it's likely that most of the dynamics are localized; i.e. lipid-free apoA-I likely exists as a discrete structure that exhibits characteristics of a molten globular protein. Thus, the model represents a time-average of those ensembles and cross-links that appear sterically hindered or solvent inaccessible likely occur on an alternate conformation within the boundaries of the experimental system. Additional studies are needed to better define these boundaries and the extent of rearrangement apoA-I can achieve *in vivo* and *in vitro*.

Finally, despite its consistency with much of the known structural data, we note that the model is still limited in resolution compared to NMR or X-ray crystallography. The general backbone configuration is likely correct, but more refined molecular interactions such as salt-bridging and hydrogen bonding are still unclear. While the protein clearly has a somewhat defined structure and shape as captured by SAXS, the exact lengths of helical domains, the precise positions of N- and C-termini and even the integrity of the helical bundle itself are likely to be in flux on the timescale of seconds. Highly unstable helices (P_f<10) that have ΔG stabilization of < 1.3 kcal/mol and are open > 10% of the time are not detected in the timescale of the H-DX kinetic experiments but are detected by CD measurements. However, truncation of the C-terminus from residue 243 to residues 221 and 231 reduces CD-detectable helix content by 14 and 7 amino acid residues, respectively[16,40]. On the basis of such observations, Mei and Atkinson[40] suggested that the segment spanning residues 231-241 contains α-helical structure. This C-terminal segment is located near the N-terminus (**Fig. 5c**) and it may contribute to the stabilization of the NT helix bundle induced by the C-terminal domain[47]. The existence of such a C-terminal helical domain is further supported by preliminary molecular dynamics simulations of the new model (Segrest et al, unpublished observation).

References

1. Silva, R.A., Hilliard, G.M., Fang, J., Macha, S. & Davidson, W.S. A three-dimensional molecular model of lipid-free apolipoprotein A-I determined by cross-linking/mass spectrometry and sequence threading. *Biochemistry* **44**, 2759-69 (2005).
2. Pollard, R.D., Fulp, B., Samuel, M.P., Sorci-Thomas, M.G. & Thomas, M.J. The conformation of lipid-free human apolipoprotein A-I in solution. *Biochemistry* **52**, 9470-81 (2013).
3. Segrest, J.P., Jones, M.K., Shao, B. & Heinecke, J.W. An experimentally robust model of monomeric apolipoprotein A-I created from a chimera of two X-ray structures and molecular dynamics simulations. *Biochemistry* **53**, 7625-40 (2014).
4. Davidson, W.S., Hazlett, T., Mantulin, W.W. & Jonas, A. The role of apolipoprotein AI domains in lipid binding. *Proc Natl Acad Sci U S A* **93**, 13605-10 (1996).
5. Bergeron, J. et al. Characterization of human apolipoprotein A-I expressed in Escherichia coli. *Biochim Biophys Acta* **1344**, 139-52 (1997).
6. Rogers, D.P. et al. Truncation of the amino terminus of human apolipoprotein A-I substantially alters only the lipid-free conformation. *Biochemistry* **36**, 288-300 (1997).
7. Sparks, D.L., Frank, P.G., Braschi, S., Neville, T.A. & Marcel, Y.L. Effect of apolipoprotein A-I lipidation on the formation and function of pre-beta and alpha-migrating LpA-I particles. *Biochemistry* **38**, 1727-35 (1999).
8. Suurkuusk, M. & Hallen, D. Denaturation of apolipoprotein A-I and the monomer form of apolipoprotein A-I(Milano). *Eur J Biochem* **265**, 346-52 (1999).
9. Davidson, W.S. et al. Structural organization of the N-terminal domain of apolipoprotein A-I: studies of tryptophan mutants. *Biochemistry* **38**, 14387-95 (1999).
10. Huang, W. et al. A single amino acid deletion in the carboxy terminal of apolipoprotein A-I impairs lipid binding and cellular interaction. *Arterioscler Thromb Vasc Biol* **20**, 210-6 (2000).
11. Panzenbock, U., Kritharides, L., Raftery, M., Rye, K.A. & Stocker, R. Oxidation of methionine residues to methionine sulfoxides does not decrease potential antiatherogenic properties of apolipoprotein A-I. *J Biol Chem* **275**, 19536-44 (2000).
12. Weinberg, R.B. et al. Structure and interfacial properties of chicken apolipoprotein A-IV. *J Lipid Res* **41**, 1410-8 (2000).
13. Sigalov, A.B. & Stern, L.J. Oxidation of methionine residues affects the structure and stability of apolipoprotein A-I in reconstituted high density lipoprotein particles. *Chem Phys Lipids* **113**, 133-46 (2001).
14. Gorshkova, I.N., Liu, T., Zannis, V.I. & Atkinson, D. Lipid-free structure and stability of apolipoprotein A-I: probing the central region by mutation. *Biochemistry* **41**, 10529-39 (2002).
15. Reschly, E.J. et al. Apolipoprotein A-I alpha -helices 7 and 8 modulate high density lipoprotein subclass distribution. *J Biol Chem* **277**, 9645-54 (2002).
16. Saito, H. et al. Domain structure and lipid interaction in human apolipoproteins A-I and E, a general model. *J Biol Chem* **278**, 23227-32 (2003).
17. Fang, Y., Gursky, O. & Atkinson, D. Structural studies of N- and C-terminally truncated human apolipoprotein A-I. *Biochemistry* **42**, 6881-90 (2003).
18. Saito, H. et al. alpha-Helix formation is required for high affinity binding of human apolipoprotein A-I to lipids. *Journal of Biological Chemistry* **279**, 20974-20981 (2004).
19. Han, J.M., Jeong, T.S., Lee, W.S., Choi, I. & Cho, K.H. Structural and functional properties of V156K and A158E mutants of apolipoprotein A-I in the lipid-free and lipid-bound states. *J Lipid Res* **46**, 589-96 (2005).
20. Zhu, X., Wu, G., Zeng, W., Xue, H. & Chen, B. Cysteine mutants of human apolipoprotein A-I: a study of secondary structural and functional properties. *J Lipid Res* **46**, 1303-11 (2005).
21. Arnulphi, C., Sanchez, S.A., Tricerri, M.A., Gratton, E. & Jonas, A. Interaction of human apolipoprotein A-I with model membranes exhibiting lipid domains. *Biophys J* **89**, 285-95 (2005).

22. Gorshkova, I.N. et al. Structure and stability of apolipoprotein a-I in solution and in discoidal high-density lipoprotein probed by double charge ablation and deletion mutation. *Biochemistry* **45**, 1242-54 (2006).
23. Tanaka, M. et al. Influence of tertiary structure domain properties on the functionality of apolipoprotein A-I. *Biochemistry* **47**, 2172-80 (2008).
24. Fukuda, M. et al. Conformational change of apolipoprotein A-I and HDL formation from model membranes under intracellular acidic conditions. *J Lipid Res* **49**, 2419-26 (2008).
25. Kono, M. et al. Disruption of the C-terminal helix by single amino acid deletion is directly responsible for impaired cholesterol efflux ability of apolipoprotein A-I Nichinan. *J Lipid Res* **51**, 809-18 (2010).
26. Chetty, P.S. et al. Helical structure and stability in human apolipoprotein A-I by hydrogen exchange and mass spectrometry. *Proc.Natl.Acad.Sci.U.S.A* **106**, 19005-19010 (2009).
27. Jayaraman, S., Cavigiolio, G. & Gursky, O. Folded functional lipid-poor apolipoprotein A-I obtained by heating of high-density lipoproteins: relevance to high-density lipoprotein biogenesis. *Biochemical Journal* **442**, 703-712 (2012).
28. Zehender, F., Ziegler, A., Schonfeld, H.J. & Seelig, J. Thermodynamics of protein self-association and unfolding. The case of apolipoprotein A-I. *Biochemistry* **51**, 1269-80 (2012).
29. Ryan, R.O., Forte, T.M. & Oda, M.N. Optimized bacterial expression of human apolipoprotein A-I. *Protein Expr Purif* **27**, 98-103 (2003).
30. Roberts, L.M. et al. Structural analysis of apolipoprotein A-I: limited proteolysis of methionine-reduced and -oxidized lipid-free and lipid-bound human apo A-I. *Biochemistry* **36**, 7615-24 (1997).
31. Rogers, D.P., Roberts, L.M., Lebowitz, J., Engler, J.A. & Brouillette, C.G. Structural analysis of apolipoprotein A-I: effects of amino- and carboxy-terminal deletions on the lipid-free structure. *Biochemistry* **37**, 945-55 (1998).
32. Barbeau, D.L., Jonas, A., Teng, T. & Scanu, A.M. Asymmetry of apolipoprotein A-I in solution as assessed from ultracentrifugal, viscometric, and fluorescence polarization studies. *Biochemistry* **18**, 362-9 (1979).
33. Edelstein, C. & Scanu, A.M. Effect of guanidine hydrochloride on the hydrodynamic and thermodynamic properties of human apolipoprotein A-I in solution. *J Biol Chem* **255**, 5747-54 (1980).
34. Mei, X. & Atkinson, D. Crystal structure of C-terminal truncated apolipoprotein A-I reveals the assembly of high density lipoprotein (HDL) by dimerization. *J Biol Chem* **286**, 38570-82 (2011).
35. Brouillette, C.G. et al. Forster resonance energy transfer measurements are consistent with a helical bundle model for lipid-free apolipoprotein A-I. *Biochemistry* **44**, 16413-25 (2005).
36. Walker, R.G. et al. The Structure of Human Apolipoprotein A-IV as Revealed by Stable Isotope-assisted Cross-linking, Molecular Dynamics, and Small Angle X-ray Scattering. *Journal of Biological Chemistry* **289**, 5596-5608 (2014).
37. Lagerstedt, J.O. et al. The "beta-clasp" model of apolipoprotein A-I--a lipid-free solution structure determined by electron paramagnetic resonance spectroscopy. *Biochim Biophys Acta* **1821**, 448-55 (2012).
38. Rogers, D.P. et al. The lipid-free structure of apolipoprotein A-I: effects of amino-terminal deletions. *Biochemistry* **37**, 11714-25 (1998).
39. Pollard, R.D., Fulp, B., Sorci-Thomas, M.G. & Thomas, M.J. High-Density Lipoprotein Biogenesis: Defining the Domains Involved in Human Apolipoprotein A-I Lipidation. *Biochemistry* **55**, 4971-81 (2016).
40. Mei, X., Liu, M., Herscovitz, H. & Atkinson, D. Probing the C-terminal domain of lipid-free apoA-I demonstrates the vital role of the H10B sequence repeat in HDL formation. *J Lipid Res* **57**, 1507-17 (2016).
41. Gursky, O. & Atkinson, D. Thermal unfolding of human high-density apolipoprotein A-1: implications for a lipid-free molten globular state. *Proc Natl Acad Sci U S A* **93**, 2991-5 (1996).

42. Melchior, J.T. et al. An Evaluation of the Crystal Structure of C-terminal Truncated Apolipoprotein A-I in Solution Reveals Structural Dynamics Related to Lipid Binding. *J Biol Chem* **291**, 5439-51 (2016).
43. Huang, B.X., Kim, H.Y. & Dass, C. Probing three-dimensional structure of bovine serum albumin by chemical cross-linking and mass spectrometry. *J Am Soc Mass Spectrom* **15**, 1237-47 (2004).
44. Jacobsen, R.B. et al. Structure and dynamics of dark-state bovine rhodopsin revealed by chemical cross-linking and high-resolution mass spectrometry. *Protein Sci* **15**, 1303-17 (2006).
45. Young, M.M. et al. High throughput protein fold identification by using experimental constraints derived from intramolecular cross-links and mass spectrometry. *Proc Natl Acad Sci U S A* **97**, 5802-6 (2000).
46. Peng, L., Rasmussen, M.I., Chailyan, A., Houen, G. & Hojrup, P. Probing the structure of human protein disulfide isomerase by chemical cross-linking combined with mass spectrometry. *J Proteomics* **108**, 1-16 (2014).
47. Koyama, M. et al. Interaction between the N- and C-terminal domains modulates the stability and lipid binding of apolipoprotein A-I. *Biochemistry* **48**, 2529-2537 (2009).